Differential pattern of HIF-1α expression in HNSCC cancer stem cells after carbon ion or photon irradiation: one molecular explanation of the oxygen effect

Anne-Sophie Wozny, Alexandra Lauret, Priscillia Battiston-Montagne, Jean-Baptiste Guy, Michael Beuve, Micaela Cunha, Yannick Saintigny, Emilie Blond, Nicolas Magné, Philippe Lalle, et al.

FULL PAPER

BJC

British Journal of Cancer (2017), 1–10 | doi: 10.1038/bjc.2017.100

Keywords: hypoxia-inducible factor-1α; carbon ion irradiation; cancer stem cells; hypoxia; reactive oxygen species; oxygen effect; photon irradiation

Differential pattern of HIF-1α expression in HNSCC cancer stem cells after carbon ion or photon irradiation: one molecular explanation of the oxygen effect

Anne-Sophie Wozny[1,2], Alexandra Lauret[1], Priscillia Battiston-Montagne[1], Jean-Baptiste Guy[1,3], Michael Beuve[1,4], Micaela Cunha[1,4], Yannick Saintigny[5], Emilie Blond[2], Nicolas Magne[1,3], Philippe Lalle[1], Dominique Ardail[1,2], Gersende Alphonse[1,2] and Claire Rodriguez-Lafrasse*[,1,2]

[1]Faculté de Médecine Lyon-Sud, Univ Lyon, Université Lyon 1, UMR CNRS5822 /IN2P3, IPNL, PRISME, Radiobiologie Cellulaire et Moléculaire, Oullins cedex F-69921, France; [2]Hospices Civils de Lyon, Centre Hospitalier Lyon-Sud, Pierre-Bénite 69495, France; [3]Département de Radiothérapie, Institut de Cancérologie de la Loire Lucien Neuwirth, St Priest en Jarez, France; [4]Univ Lyon, Université Lyon 1, UMR CNRS5822 /IN2P3, IPNL, PRISME, PHABIO, Villeurbanne 69322, France and [5]Laboratoire de Radiobiologie Cellulaire Moléculaire -Commissariat à l'Energie Atomique et aux Energies Alternatives, Fontenay aux Roses 92265, France

Background: Head and neck squamous cell carcinoma (HNSCC) are resistant to standard treatments, partly due to cancer stem cells (CSCs) localised in hypoxic niches. Compared to X-rays, carbon ion irradiation relies on better ballistic properties, higher relative biological effectiveness and the absence of oxygen effect. Hypoxia-inducible factor-1α (HIF-1α) is involved in the resistance to photons, whereas its role in response to carbon ions remains unclear.

Methods: Two HNSCC cell lines and their CSC sub-population were studied in response to photons or carbon ion irradiation, in normoxia or hypoxia, after inhibition or not of HIF-1α.

Results: Under hypoxia, compared to non-CSCs, HIF-1α is expressed earlier in CSCs. A combined effect photons/hypoxia, less observed with carbon ions, results in a synergic and earlier HIF-1α expression in both subpopulations. The diffuse ROS production by photons is concomitant with HIF-1α expression and essential to its activation. There is no oxygen effect in response to carbon ions and the ROS localised in the track might be insufficient to stabilise HIF-1α. Finally, in hypoxia, cells were sensitised to both types of radiations after HIF-1α inhibition.

Conclusions: Hypoxia-inducible factor-1α plays a main role in the response of CSCs and non-CSCs to carbon ion and photon irradiations, which makes the HIF-1α targeting an attractive therapeutic challenge.

Head and neck squamous cell carcinoma (HNSCC) is the sixth leading cause of cancer worldwide. Treatments are based on the use of surgery, chemotherapy, radiotherapy, alone or in combination. Despite improvements of these therapeutic tools, loco-regional recurrence rates remain very high, up to 30–50% at 5 years (Li *et al*, 2014). Solid tumours are often considered as organ-like structures, composed of heterogeneous cell populations. A complex network of cytokines and growth factors regulate their poorly vascularised microenvironment and many factors contribute to the development of an intrinsic radioresistance. Resistance

*Correspondence: Professor C Rodriguez-Lafrasse; E-mail: claire.rodriguez-lafrasse@univ-lyon1.fr

Received 9 March 2017; revised 17 March 2017; accepted 21 March 2017

to treatment partly results from the existence of poorly oxygenated areas within the tumour, thus creating a microenvironment, which helps ensuring a physical barrier to cancer cells, but also plays a protective role against chemo- and radiotherapy treatments (Peitzsch *et al*, 2014). The correlation between the low oxygen concentrations in the tumour and the poor clinical outcome after photon radiotherapy has been previously reported in HNSCC solid tumours (Nordsmark *et al*, 2005). Furthermore, a sub-population of cells, the cancer stem cells (CSCs), initially found in leukemia cells (Lapidot *et al*, 1994) are preferentially localised in hypoxic niches (Ye *et al*, 2014). Cancer stem cells are particularly involved in resistance to treatment, proliferation, migration process, invasiveness and metastasis, and interplay closely with their microenvironment. Hypoxia has a main role in their self-renewal and in the maintaining of their stemness (Das *et al*, 2008). Cancer stem cells and non-CSCs are known to have very different properties, mainly due to their phenotype, that is, mesenchymal for CSCs and epithelial for non-CSCs. Furthermore, HNSCC-CSCs have higher invasiveness and migration properties compared to non-CSCs (Moncharmont *et al*, 2016). Currently, CSCs are supposed to be partially responsible for relapses observed after photon irradiation (Rycaj and Tang, 2014). Furthermore, when cells are irradiated with photons under various levels of oxygenation, the radiosensitivity increases with the oxygen concentration (Tonissi *et al*, 2016). Indeed, oxygen plays an essential role in the response to ionising radiation through the production of ROS induced by water radiolysis.

Hadrontherapy is considered as an alternative to overcome the intrinsic radioresistance of CSCs (Tobias *et al*, 1982). Owing to their high linear energy transfer (LET), carbon ions have optimal properties in terms of physical dose distribution. Unlike photons with which the dose is progressively deposited as a function of the penetration depth in the body, according to an uniform pattern of distribution, carbon ions are able to deposit most of their energy at the end of the track, during the Bragg peak. This ballistic precision allows to use this technology to target deep-seated tumours while sparing the surrounding healthy tissues and organs at risk (Levin *et al*, 2005). Additionally, due to their high LET, they have a higher relative biological effectiveness (RBE) compared to photons, inducing severe DNA damage localised around the particle track that are more complex to repair (Prise *et al*, 1994). Carbon ions have also been reported to be more deleterious on CSCs (Bertrand *et al*, 2014). Another important advantage of hadrontherapy is that carbon ions, at the opposite of photons, act independently of the oxygen concentration. Some physical theories have then been developed and argue that heavy ions could produce molecular oxygen in the track that could compensate the lack of oxygen (Dettmering *et al*, 2015). In fact, due to their close proximity, the hydrogen radicals interact between each other in the track to form oxygen (Colliaux *et al*, 2011). However, concerning the molecular mechanism involved, there is up to now only a few data concerning the CSCs response to photon and carbon ion irradiations, even more under hypoxia, and the mechanisms have to be clarified in HNSCC, particularly for the CSCs.

Under hypoxia, the protein hypoxia-inducible factor-1 (HIF-1) is considered as the major transcriptional regulator of the cellular and developmental response to oxygen homeostasis. Hypoxia-inducible factor-1 is a heterodimeric protein, consisting of two subunits: the oxygen-sensitive HIF-1α and the constitutively expressed HIF-1β (Semenza, 2001). Under oxic conditions, the propyl hydroxylase enzymes hydroxylate two proline residues of the HIF-1α subunit, which allow the von Hippel-Lindau tumour suppressor protein (pVHL) to bind to HIF-1α and target it to proteasome for degradation (Rankin and Giaccia, 2016). During hypoxia, mitochondria increase their ROS production, inducing the inhibition of propyl hydroxylase activity, thus leading to HIF-1α stabilisation. Then, the HIF-1α/HIF-1β complex translocates to the nucleus and induces the transcription of many genes involved in the cellular adaptation to hypoxia, such as those related to angiogenesis, erythropoiesis, cell proliferation, survival and the glucose and iron metabolism (Ke and Costa, 2006). Hypoxia-inducible factor-1α could also be stabilised in response to various cellular stress such as photon irradiation (Subtil *et al*, 2014). The molecular mechanisms which enable HIF-1α induction in response to photon irradiation depend partly on the Akt/mTOR signalling pathway (Harada *et al*, 2009). Moreover, Ogata *et al* (2011) showed that photon irradiation enhances the phosphorylation of Akt, whereas carbon ion irradiation decreases it, leading to the inhibition of HIF-1α expression in human lung adenocarcinoma cell line under normoxia. More recently, a DNA microarray study in adenocarcinoma demonstrated that the mTOR pathway was significantly altered after photon but not carbon ion irradiation (Subtil *et al*, 2014). Although photons increase the phosphorylation of the mTOR protein, this study reported that carbon ion irradiation decreases significantly its phosphorylation, leading to the inhibition of HIF-1α expression. Nevertheless, the role of ROS in the mechanisms of HIF-1α induction after carbon ion exposure particularly under hypoxia, is poorly understood and need to be clarified.

The objective of this work was thus to determine the role of HIF-1α in response to carbon ion irradiation compared with photons, in normoxic and hypoxic conditions, with a particular focus on CSCs, which are localised in hypoxic niches.

MATERIALS AND METHODS

Cell culture. SQ20B and FaDu radioresistant cell lines were established from HNSCC tumour and provided by J Little (Boston, MA, USA) and ATCC (Manassas, VA, USA), respectively. SQ20B as well as its sub-population of cancer stem cells SQ20B-CSCs were cultured as previously described (Bertrand *et al*, 2014). FaDu and FaDu^{CD44low} cell lines were maintained at 37 °C with 5% CO_2 in MEM (Life Technologies, Paisley, UK) supplemented with 10% fetal bovine serum (FBS) (100 U ml^{-1} penicillin, 0.1 g l^{-1} streptomycin, Life Technologies), 1% of sodium pyruvate and amino-acids (GE Healthcare, Little Chalfont, UK). For FaDu-CSCs, medium contained only 5% of FBS and a supplementation with 20 ng ml^{-1} of epidermal growth factor (Eurobio, Les Ulis, France). Hypoxic conditions were obtained in a tri-gaz chamber (Heracell 150i, Thermo, Waltham, MA, USA) under an atmosphere containing 1% O_2, 5% CO_2 and 94% N_2 at 37 °C.

Cells were maintained in chronic hypoxia with several passages in hypoxic conditions or incubated in acute hypoxia from 30 min to 24 h for kinetic studies.

CSCs isolation. SQ20B-CSCs were obtained after two successive cells sorting (Hoechst efflux and CD44/ALDH labeling) as described by (Gilormini *et al*, 2016). Tumoursphere formation, quantification of stemness markers expression and tumourigenicity *in vivo* were validated for both CSCs. The parental SQ20B cell line, named SQ20B^{CD44low}, which contains $<1\%$ of CSCs was chosen as the negative control for comparative experiments. FaDu^{CD44low} cells, obtained after cell sorting, were used as the negative control since the FaDu parental cell line contains 20–30% of CD44-positive cells (Shen *et al*, 2013).

Transient transfection. For transfection experiments, a SiRNA targeting HIF-1α (exon 5), an irrelevant siRNA as a negative control, or a FITC-labeled siRNA (ThermoFisher, Rockford, IL, USA) were used. Cells were trypsinised, then diluted at 10^5 cells per ml and 2 ml per well of cell suspension were distributed in a 24-wells plate. A mix composed of 1.36 μl ml^{-1} of HighPerFect (Qiagen, Hilden, Deutschland) and 0.16 μl ml^{-1} of the siRNA QSP 500 μl (MEM or DMEM function of the cell line) was added in

each well and incubated 15 min at room temperature. Cells were then incubated overnight at 37 °C, under normoxic or hypoxic conditions, before experiments. In order to control the transfection efficiency, cells transfected with the FITC-labeled siRNA were analysed by FACS (BD, LSRII) the day of the experiment. The extinction of HIF-1α expression was also confirmed by western blot (Supplementary Data S1).

Photon and carbon ion irradiations. Photon irradiations (250 kV) and carbon ion irradiation (72 MeV/n LET: 33.6 keV μm^{-1} GANIL, Caen, France) (Durantel *et al*, 2016) were performed as previously described (Beuve *et al*, 2008). All experiments were performed at equivalent physical dose for irradiations as recommended by Kamada *et al* (2015).

Colony formation assay. Cell survival curves were assessed by the standard colony formation assay as described in Beuve *et al* (2008). Colonies containing at least 64 cells were counted with a Colcount system (Optronix, Oxford, UK). Survival curves were calculated according to the formula of the linear quadratic model $S = \exp(-\alpha D - \beta D^2)$, where S is the survival fraction and D the dose in Gray. For carbon ion irradiations, the curves were fitted with $S = \exp(-\alpha D)$. The oxygen enhancement ratio (OER) was determined as the ratio of the dose leading to 10% survival (D_{10} values) for chronic hypoxia *versus* normoxic conditions.

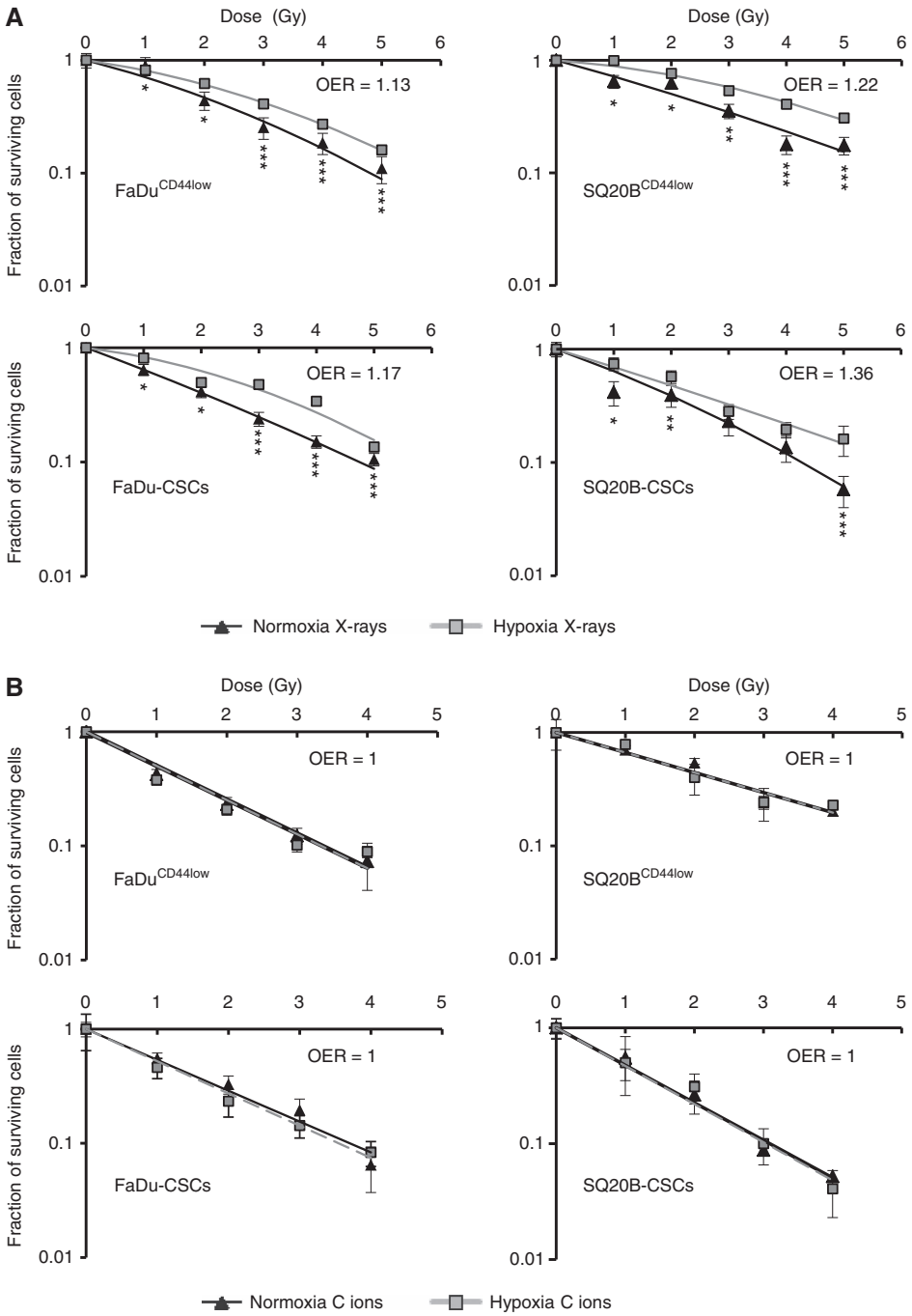

Figure 1. Clonogenic survival curves. FaDu^{CD44low}, SQ20B^{CD44low}, FaDu-CSCs and SQ20B-CSCs were exposed to photons (**A**) or carbon ion (**B**) irradiation in normoxic conditions (21% O_2) or chronic hypoxia (1% O_2). Values represent the mean ± s.d. of three (**A**) or two (**B**) independent experiments performed in sextuplicate. Student's *t*-test was performed between survival fractions of normoxia and hypoxia curves for each cell lines (*$P<0.05$, **$P<0.01$ and ***$P<0.005$).

Western blot analysis. Cells treated 16 h with 200 μM cobalt salts were used as a HIF-1α-positive control. For the experiments with a ROS scavenger, 1% dimethyl sulfoxyde (DMSO) was added to cells 1 h before irradiation. Cells were placed under hypoxia and/or irradiated at $t = 0$ h and immediately incubated under oxic or hypoxic conditions during 30 min to 24 h before cell lysis. Proteins were separated on 10% polyacrylamide gels and transferred onto nitrocellulose membrane. The monoclonal antibodies used were as follows: anti-HIF1α (1 : 500), anti-GAPDH (1 : 100 000) (BD Transduction, San Jose, CA, USA) and anti-HRP (1 : 7000) (Santa Cruz, Dallas, TX, USA). Western-blots signals were measured by densitometric scanning with an Azure C300 Intelligent Dark Box (Biosystems Inc, Dublin, CA, USA) and protein expressions were quantified with MultiGauge (FujiFilm, Tokyo, Japan) after GAPDH normalisation (Figures 2A, 5B and D).

Detection of intracellular reactive oxygen species (ROS). Cells were plated at 2.10^5 cells per well of a 24-well plate. After irradiation and/or acute hypoxia from 30 min to 24 h, cells were washed with PBS, and then incubated 10 min at 37 °C in the dark with 2.5 μM CM-H_2DCFDA (ThermoFisher Scientific, Rockford, IL, USA), which stains H_2O_2, HO·, ROO· and $ONOO^-$. Cells were then washed with PBS, trypsinised and a minimum of 10 000 cells per sample were analysed using a FACS-BD-LSRII. The median fluorescence intensity was calculated for each sample using the DiVa software (BD).

Determination of the reduced glutathione concentrations. Reduced glutathione (GSH) was quantified by high performance liquid chromatography and mass spectrometry (HPLC-MS, Agilent Technologies, Venissieux, France) (Revel *et al*, 2015). After irradiation and/or acute hypoxia from 30 min to 24 h, cells were incubated 30 min at room temperature with 200 μl of a solution containing 20 mM N-ethylmaleimide, 2 mM EDTA, 250 μM L-glutamyl-L-glutamic acid (internal standard) and 1.5% sulfosalicylic acid. Wells were scratched and transferred into 1.5 ml Eppendorf vials before centrifugation at 15 000 g, 15 min at 4 °C. Supernatants were used to measure GSH levels. Chromatograms were then integrated using the Chemstation software.

Statistical analysis. Student's *t*-test was used to compare difference between groups. *P*-values lower than 0.05 ($P < 0.05$) were considered to be statistically significant. $^*P < 0.05$; $^{**}P < 0.01$ and $^{***}P < 0.005$.

RESULTS

Impact of hypoxia on cell survival in response to carbon ion and photon irradiations. Cell survival curves for the FaDu^{CD44low} and SQ20B^{CD44low} cell lines as well as for FaDu-CSCs and SQ20B-CSCs were established after photon irradiation in normoxic and chronic hypoxic conditions (Figure 1A). The radiobiological parameters α, β, D_{10} values, RBE (relative biological effectiveness at 10% survival) and oxygen enhancement ratio (OER) at 10% survival obtained are listed in the Supplementary Data S2A. The statistical differences were calculated for each dose point between oxic and hypoxic conditions. As expected, after photon irradiation, the four HNSCC cell lines were significantly more resistant under hypoxia compared to normoxia. For the FaDu^{CD44low} cells, the dose delivered for 10% of survival (D_{10}), increased from 4.7 Gy in normoxia to 5.4 Gy in hypoxia (OER: 1.15) (see Supplementary Data S2A). For FaDu-CSCs, the D_{10} shifted from 4.9 Gy in normoxia to 5.7 Gy in hypoxia (OER: 1.17). The OER for SQ20B^{CD44low} and SQ20B-CSCs were 1.22 and 1.36, respectively. The better efficiency of carbon ions compared to photons was confirmed by the survival curves (Figure 1B). Moreover, an OER of 1 was found for all the cells.

Influence of carbon ion and photon irradiations on HIF-1α protein expression. The kinetic of HIF-1α expression was assessed after photon or carbon ion exposure, in normoxia or acute hypoxia. The expression profile of HIF-1α was studied at 10 Gy photons, 10 Gy (physical dose) and 5 Gy (biological equivalent dose) carbon ions (Figure 2; Supplementary Data S3). Under hypoxia, the expression of HIF-1α was maximal at 6 h in FaDu^{CD44low} and SQ20B^{CD44low} cell lines (line A), whereas this maximal was around 2 h for FaDu-CSC and SQ20B-CSC populations. For all the cell lines, after the peak, the expression of HIF-1α decreased until 24 h. After a 10 Gy photon exposure in normoxia (line B), the expression of HIF-1α increased from 1 h, peaked at 2 h and then decreased in the FaDu^{CD44low} cell line. For SQ20B^{CD44low} cells, this expression was later (4 h). Regarding both CSC cell lines, the expression of HIF-1α is less marked and started from 30 min up to 2 h. When cells were exposed to photon exposure under hypoxic conditions (line C), the expression of HIF-1α was stronger and mostly earlier compared to normoxia. After carbon ion exposure under normoxia (line D), whatever the dose used (5 or 10 Gy), and unlike photons, a lack of HIF-1α

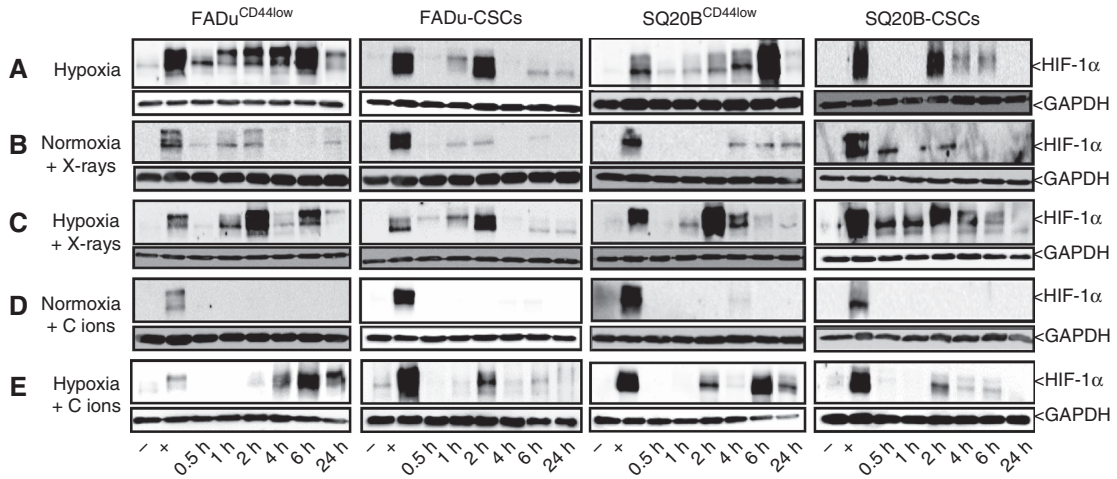

Figure 2. Kinetics studies of HIF-1α expression. FaDu^{CD44low}, SQ20B^{CD44low}, FaDu-CSCs and SQ20B-CSCs cell lines were exposed to 10 Gy of photon or carbon ion irradiation under normoxia (respectively lines **B** and **D**) or acute hypoxia (line **C** and line **E**, line **A** for hypoxia alone). Kinetic studies from 30 min to 24 h were realised ($n = 3$). The reference time was defined when cells were irradiated and/or placed under hypoxia. Forty micrograms of proteins were loaded on western blots and GAPDH was used as a reference protein. Positive and negative controls were realised with cells incubated 16 h in normoxia respectively after treatment with or without 200 μM cobalt salts.

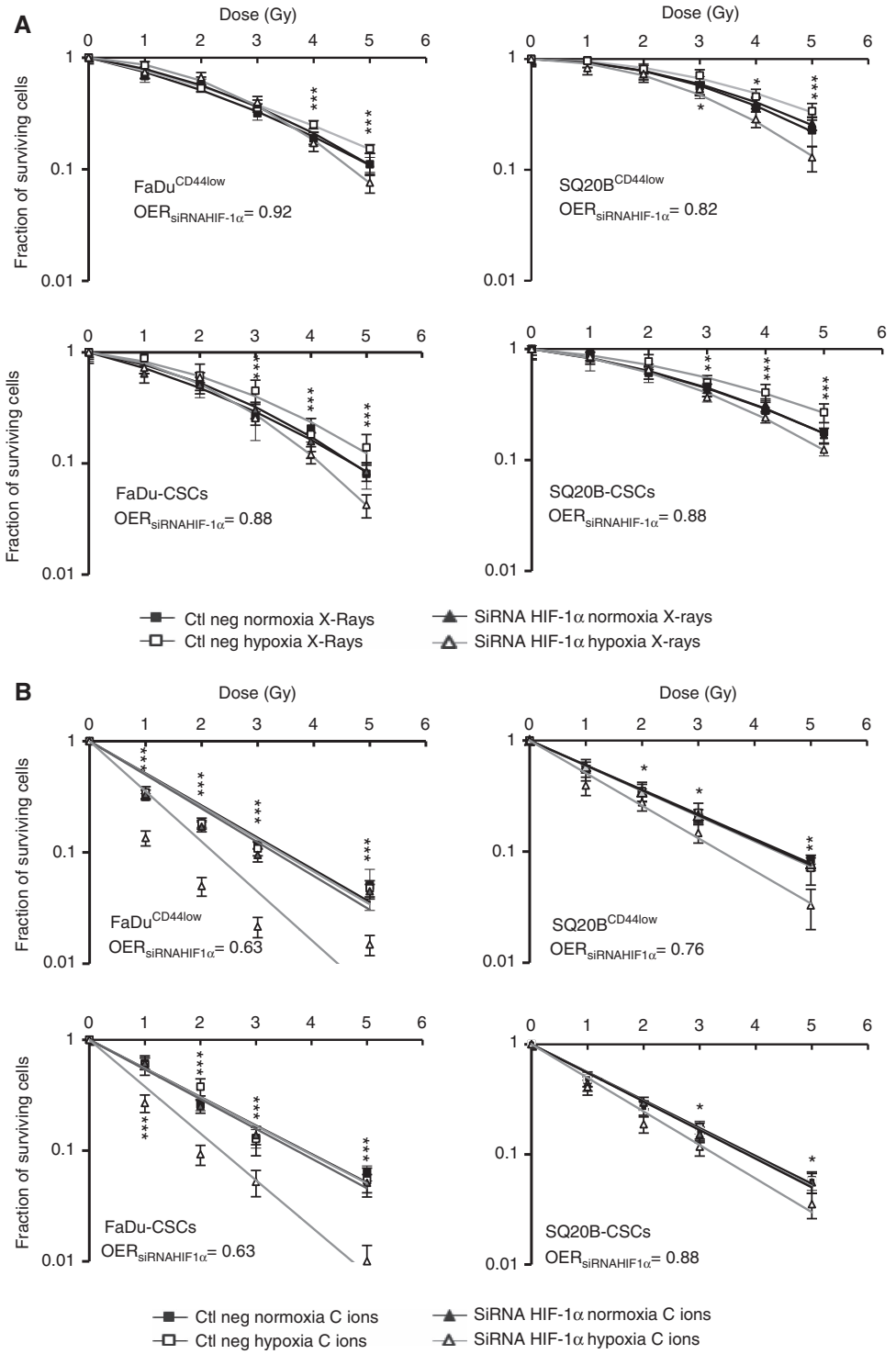

Figure 3. Clonogenic survival curves after cell transfection with a siRNA targeting HIF-1α or an irrelevant siRNA. FaDu^{CD44low}, SQ20B^{CD44low}, FaDu-CSCs and SQ20B-CSCs cell lines were transfected with the siRNA of interest and exposed to photons (**A**) or carbon ions (**B**) in normoxic or hypoxic conditions. Square and triangle plots represent respectively the negative control and the siRNA survival fraction. Black plots are for normoxia and open plots for hypoxia. Values represent the mean ± s.d. of two independent experiments performed in sextuplicate. Student's *t*-test was performed between the survival fractions of ctl neg hypoxia and siRNA HIF-1α hypoxia curves for each cell lines (*$P<0.05$, **$P<0.01$ and ***$P<0.005$). The OER was calculated at 10% of surviving cells for both the cell lines transfected with the siRNA HIF-1α.

stabilisation was observed for the four cell lines. Irradiation with carbon ions under hypoxia (line E) induces similar results to those obtained under hypoxia alone: a maximal expression of HIF-1α at 6 h for the non-CSCs and 2 h for the corresponding CSCs. However, the levels of expression remain lower than those obtained under hypoxia alone, which exclude a synergy between these two experimental conditions. Our results clearly show that HIF-1α is expressed in response to photons and under hypoxia whatever the experimental conditions used, whereas under normoxia, carbon ion exposure did not stabilised HIF-1α.

Consequences of the inhibition of HIF-1α on the radioresistance of the HNSCC cell lines. To go further in understanding the role of HIF-1α in the response to radiation, siRNA experiments targeting HIF-1α were undertaken and cell survival curves were established with or without inhibition of HIF-1α (Figure 3 and Supplementary Data S2B). Control experiments showed that ~80% of cells were transfected for the FaDu^{CD44low} cell lines (Suplementary Data S1) and no expression of the protein was observed with the siRNA targeting HIF-1α, unlike cells treated with the irrelevant siRNA associated to $CoCl_2$. In response to photons, cells under hypoxia and transfected with the irrelevant siRNA (curves with white square), were associated to an oxygen effect (OER > 1) (Figure 3A). At the opposite, no difference occurred in the surviving fraction of the four cell lines transfected with the irrelevant siRNA after carbon ion irradiation under hypoxia compared to normoxia (OER = 1) (Figure 3B). The inhibition of HIF-1α expression, under hypoxia (curves with white triangle in Figure 3A and B), resulted in a significant radiosensitisation of the four cell lines to both photon and carbon ion irradiations (OER < 1). The OER were calculated between the D_{10} values of cells transfected with the HIF-1α siRNA in normoxia and the one transfected with the HIF-1α siRNA in hypoxia. Statistical analysis was performed between each ctl neg hypoxia (white square plots) and siRNA hypoxia (white triangle) dose points. These results clearly show the involvement of HIF-1α after both types of irradiations in hypoxic conditions.

Redox status and activation of HIF-1α. In order to improve our knowledge about the mechanisms leading to HIF-1α stabilisation in response to photon compared to carbon ion irradiation, the

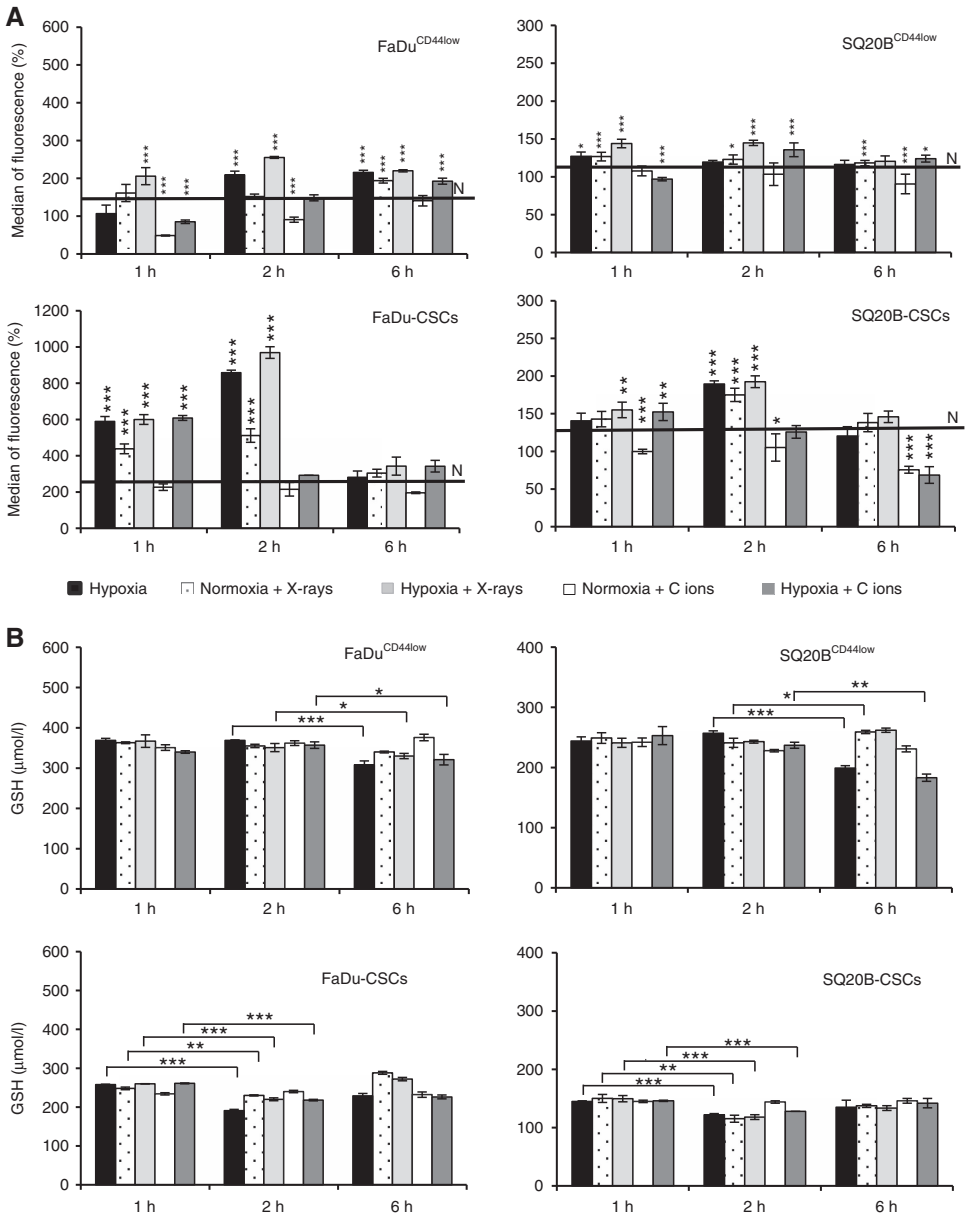

Figure 4. Evaluation of the REDOX status. FaDu^{CD44low}, SQ20B^{CD44low}, FaDu-CSCs and SQ20B-CSCs cell lines were cultured under hypoxia or normoxia (black line N) after photon or carbon ion exposure. (**A**) Relative increase of the ROS production at the key times points corresponding to HIF-1α expression, compared to normoxia (N). (**B**) Reduced glutathione concentrations were quantified by HPLC-SM and were represented for the four populations of HNSCC studied. Values represent the mean ± s.d. of three (**A**) and two (**B**) independent experiments performed in triplicate. A student's *t*-test was performed for **A** values (between ROS of interest and reference value under normoxia) and for **B** (between GSH concentrations at 2 and 6 h for non-CSCs and 1 and 2 h for CSCs). *$P < 0.05$; **$P < 0.01$ and ***$P < 0.005$.

redox status (ROS production and reduced GSH concentrations) was studied (Figure 4 and Supplementary Data S4). In basal conditions (black line N (Normoxia) on each figure), ROS levels (Figure 4A) were significantly lower in non-CSCs compared to CSCs with a value of 123 ± 18% and 113 ± 6% positive cells for $FaDu^{CD44low}$ and $SQ20B^{CD44low}$ against 280 ± 22% and 127 ± 5% for FaDu-CSCs and SQ20B-CSCs, respectively. Under hypoxia alone (black bars) and for photons (white dotted bars), hypoxia/photons (light grey bars) or hypoxia/carbon ion irradiation (dark grey bars), ROS increased was shown at 6 h for non-CSCs and 2 h for CSCs before going back to normoxia values. At 24 h, a late ROS production was observed in the four cell lines (Supplementary Data S4). In light of these results, the peak of ROS appeared to correlate with the maximum of HIF-1α expression, that is, between 4 and 6 h for low CD44 cell lines and 2 h for CSCs. Statistics were performed between the value of interest and the value of reference under normoxia (black line N).

Reduced glutathione concentrations (GSH) were also measured after irradiation at the key times of HIF-1α expression (Figure 4B). Statistics were calculated between 1 h and 2 h values for CSCs and between 2 and 6 h for the non-CSCs, which correspond to the peak of ROS expression. Our results confirmed that ROS

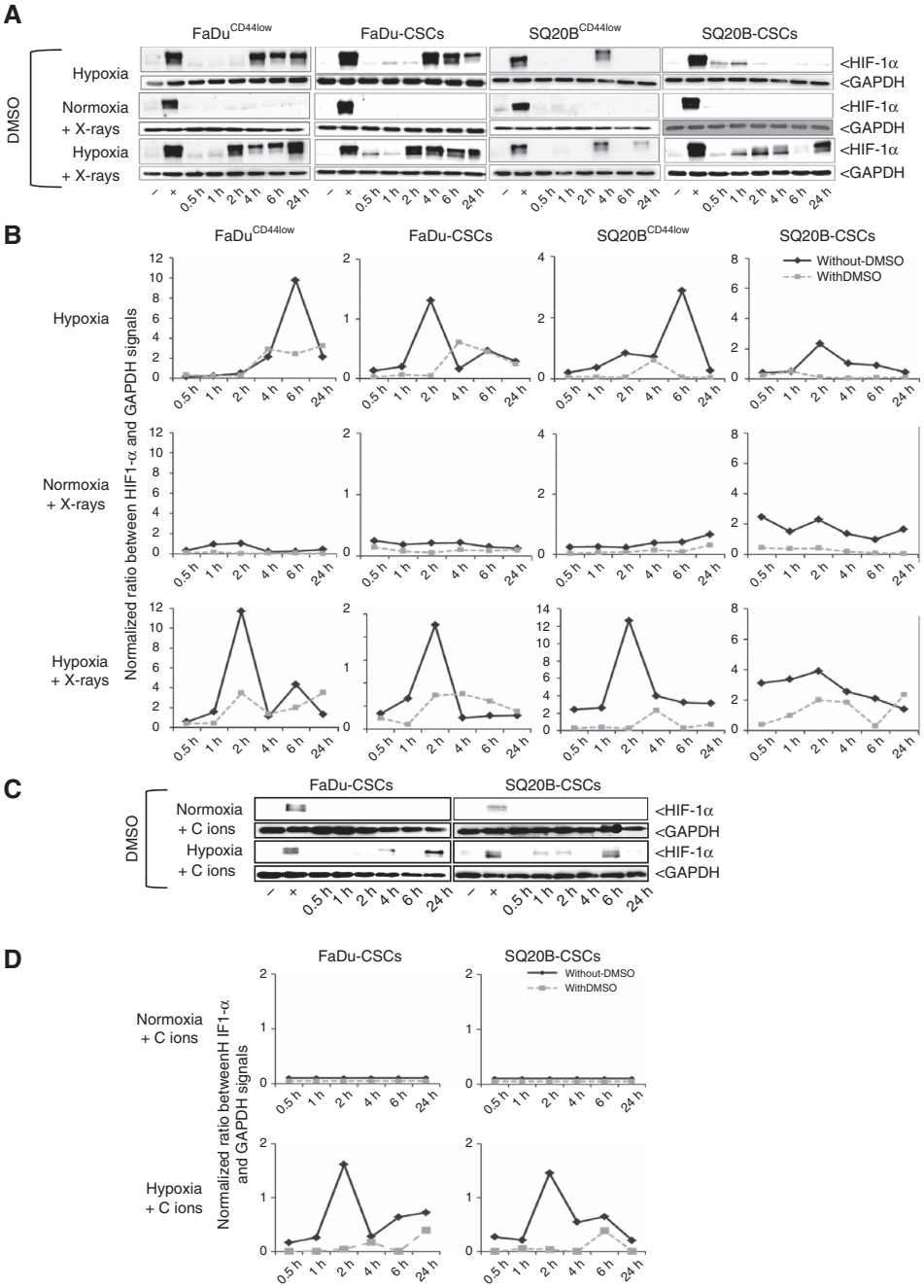

Figure 5. Consequences of the inhibition of ROS production on the activation of HIF-1α. (**A**) Western blot study of HIF-1α expression after 1% DMSO treatment in the four HNSCC populations after X-rays. (**B**) Expression of HIF-1α quantified and normalised to GAPDH with DMSO in dotted line (**A**) or without DMSO treatment in full line (WB in Figure 2). (**C**) Kinetic study of HIF-1α expression after DMSO treatment in FaDu-CSCs and SQ20B-CSCs after carbon ion irradiation. (**D**) Comparison of the HIF-1α expression quantified and normalised to GAPDH after carbon ion irradiation with DMSO in dotted line (**C**) or without DMSO treatment in full line (WB in Figure 2).

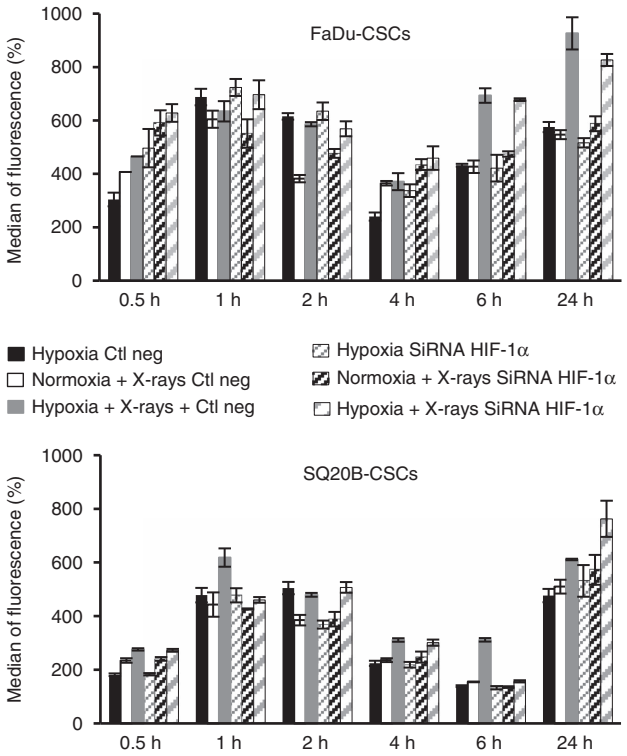

Figure 6. Influence of HIF-1α on ROS production in FaDu-CSCs and SQ20B-CSCs. Both CSC cell lines were transfected with an irrelevant siRNA or a siRNA targeting HIF-1α and the ROS production was measured with the CM-H_2DCFDA dye and analysed by FACS under hypoxia or after 10 Gy photons in normoxic or hypoxic conditions from 30 min to 24 h. Values represent the mean ± s.d. Globally, no differences were observed between cells transfected with the siRNA against HIF-1α and the irrelevant siRNA. *$P<0.05$; **$P<0.01$ and ***$P<0.005$.

production is thus concomitant with the intracellular concentration of GSH, since when ROS production increases, GSH concentration decreases and conversely but also with HIF-1α kinetic expression.

Consequences of a ROS inhibition on the HIF-1α expression. To determine the role of the ROS production in the potential activation of HIF-1α, DMSO, a ROS scavenger, was used (Figure 5) and kinetics of protein expression were studied. Figure 5 shows a decrease of HIF-1α expression after DMSO treatment under hypoxia with or without photons (Figure 5A) or after carbon ion irradiations (Figure 5C) in the four cell lines studied. Respective HIF-1α expressions were quantified (Figures 5B and D) and compared to HIF-1α expressions without DMSO treatment (Figure 2). These results put in evidence the main role of the ROS production in the HIF-1α activation.

Impact of the inhibition of HIF-1α expression on the ROS production. In these experiments, the production of ROS was measured after transfection with an irrelevant SiRNA or SiRNA targeting HIF-1α from 30 min to 24 h under hypoxia alone or after 10 Gy photons in normoxic or hypoxic conditions. Cells transfected with the negative control (Figure 6) present the same profile as non-transfected FaDu-CSCs and SQ20B-CSCs cells with a peak of ROS production between 1 and 2 h and a late ROS production at 24 h, whatever the experimental conditions used. After HIF-1α SiRNA transfection, no significant difference in the fluorescence intensity was observed in both CSCs cell lines, thus suggesting that inhibition of HIF-1α expression has no influence on the ROS production.

DISCUSSION

Understanding the involvement of the oxic conditions on the response of CSCs to carbon ion exposure compared to photons is essential to improve therapeutic care and overcome resistance. To that end, the first part of this study was to determine the influence of oxygen concentration on the radioresistance of HNSCC to photon and carbon ion exposure with specific attention to CSCs. As expected, and previously reported in CHO-K1 (Antonovic *et al*, 2013), we observed in HNSCC cell lines on one hand that hypoxia induces radioresistance after photon exposure, thus leading to an OER >1 and on the other hand, that the absence of oxygen effect for FaDu^{CD44low} and SQ20B^{CD44low} cell lines (OER $=1$) in response to carbon ion exposure (Wenzl and Wilkens, 2011). These observations were confirmed with cells transfected with the negative control in response to both irradiations. This finding supports the postulate that the OER decreases as the LET increases (Tinganelli *et al*, 2015). More interestingly, we showed that unlike photon exposure, carbon ion irradiation can overcome the effect of hypoxia in both subpopulations of CSCs, FaDu-CSCs and SQ20B-CSCs (OER $=1$). These results highlight the great efficiency of carbon ion on CSCs both in normoxic (Schlaff *et al*, 2014) and hypoxic conditions.

The cellular response to hypoxia is based on the expression of the protein HIF-1α. HIF-1α is involved in the activation of many signalling pathways inducing apoptosis, cell survival, stem cell properties or metastasic process (Polyak and Weinberg, 2009). In this work, we showed in the parental and CSC cell lines that HIF-1α is always expressed under hypoxia, whatever the type of irradiation used, whereas no expression was found in normoxic conditions and after carbon ion exposure. Furthermore, photon irradiation coupled with hypoxic conditions had a synergistic effect on HIF-1α expression. Our results also underlined that HIF-1α expression began at an earlier stage in CSC cell lines compared to non-CSCs, thus suggesting that CSCs already have adaptive properties to hypoxia (Myszczyszyn *et al*, 2015). In this sense, it has been recently demonstrated that hypoxia maintains CSCs properties in ovarian cancer (Seo *et al*, 2016). Generally, HIF-1α is revealed a few hours after hypoxia exposure and because of its small half-time (5–7 min), is no more expressed after coming back to normoxia (Wulbrand *et al*, 2013). Even though hypoxia is the main condition by which HIF-1α is stabilised, there is also non-hypoxic stimuli like ionising radiation, which avoid HIF-1α to be addressed to the proteasome (Kim *et al*, 2014). At the opposite, Subtil *et al*, 2014 have showed in adenocarcinoma cells lines, that carbon ions could totally inhibit HIF-1α stabilisation by decreasing mTOR phosphorylation but this process was not studied in CSCs. Then, under hypoxia, the difference in the kinetics of HIF-1α expression in response to photons compared to carbon ions may partly explain the difference of OER obtained.

In order to demonstrate the role of HIF-1α in the response to high or low LET irradiation, the impact of its inhibition on cell survival was investigated. It was previously shown that inhibition of HIF-1α induces a radiosensitisation of HNSCC cells in hypoxia after photon exposure (Fu *et al*, 2015), a result that we have confirmed in this study for FaDu^{CD44low} and SQ20B^{CD44low}. Interestingly, the same results were obtained for the FaDu-CSCs and SQ20B-CSCs cell lines. On the other hand, as a stabilisation of HIF-1α was demonstrated in response to carbon ion irradiation under hypoxia (Figure 2), its inhibition induces a sensitisation of the cells, particularly the CSCs. Consequently, we confirmed the essential role of HIF-1α in the radioresistance induced by photons (Jin *et al*, 2015) but also demonstrated its involvement in the response to carbon ion irradiation under hypoxia and mostly in the populations of CSCs. Subtil *et al* have (2014) already suggested that mTor phosphorylation, which is not observed in response to

carbon ion under normoxia could be essential to HIF-1α activation. A difference in the signalling pathway activated could explain the radiosensitisation observed in response to carbon ions.

It is well established that ROS are involved in the activation of HIF-1α (Movafagh *et al*, 2015) and some data also imply HIF-1α in glutathione biosynthesis (Lu *et al*, 2015). Furthermore, there is a late ROS production from 24 h, as described previously and possibly resulting of the mitochondrial dysfunction during activation of the apoptosis (Boivin *et al*, 2011). In the four cell lines studied, particularly for FaDu-CSCs and SQ20B-CSCs, ROS production and HIF-1α expression were concomitant in response to both types of irradiations in normoxia or hypoxia, which seems to confirm the direct role of ROS on HIF-1α expression. Reduced glutathione levels measurements were found to be inversely correlated with ROS production and HIF-1α expression, that is, a significant decrease at 2 h for CSCs and 6 h for non-CSCs, particularly in hypoxic conditions. One potential explanation of the role of oxygen in the response to radiations could be the involvement and the localisation of ROS. Although DNA damage after low-LET photon exposure relies mainly on the diffuse indirect oxygen-dependent effect, the production of ROS is localised in the carbon ion track, leading to their recombination and annihilation, which should explain the lack of oxygen effect (Meesungnoen and Jay-Gerin, 2009). Indeed, the proportion between direct and indirect effects is discussed since a long time (Douki *et al*, 2006). Additionally, under hypoxia, electrons can accumulate in the mitochondria compartment and induce the reduction of O_2 molecules into $O_{2^-}\cdot$ radicals. Reactive oxygen species are then produced by mitochondrial complexes responsible for stabilising HIF-1α during hypoxia (Lu *et al*, 2015). Although the mechanisms involved in the oxygen effect remains up to now largely unclear, particularly in response to carbon ion irradiation, the differences in the ROS distribution independent of the oxygen concentration could explain the difference in HIF-1α stabilisation.

In order to understand if ROS production is a cause or a consequence of HIF-1α activation, ROS inhibition experiments were undertaken. As a consequence of this inhibition, for the non-CSCs and CSCs, HIF-1α expression was downregulated in response to photon in both oxic and hypoxic conditions. In response to carbon ion exposure, inhibition of ROS led also to a significant decrease of HIF-1α expression under hypoxia. Consequently, localised ROS after carbon ion exposure seems to play a role in the activation of HIF-1α in hypoxia, including CSCs. All these results confirm that ROS are involved in the activation of HIF-1α after photon exposure both in normoxia and hypoxia but also in response to carbon ion irradiation in hypoxia (Supplementary Data S5).

The specific targeting of HIF-1α remains an important challenge in oncology. Numerous studies have been undertaken to inhibit HIF-1α at different levels such as HIF-1α mRNA expression, HIF-1α translation, stabilisation or dimerization, DNA binding or transcriptional activity inhibition (Masoud and Li, 2015). Wang *et al* (Wang *et al*, 2016) showed that the inhibition of the PI3K/Akt/mTor pathways with bufalin led to a decrease of the HIF-1α expression correlated to a decrease of invasion in hepatocellular carcinoma. Another study demonstrated that inhibition of HIF-1α/*β* dimerisation have an adjuvant effect with photodynamic therapy to sensitise cholangiocarcinoma (Weijer *et al*, 2016). Up to now, the mechanism linking HIF-1α and carbon ion irradiation has not been elucidated, even less for CSCs. In that sense, we present evidence for a major role played by HIF-1α, through ROS production, in the resistance of HNSCC and related CSCs in response to photon as well as carbon ion irradiation under hypoxia. Inhibition of HIF-1α coupled to radiation and preferentially carbon ions could be an attractive therapeutic strategy to effectively target CSCs and therefore overcome radioresistance as well as recurrence.

ACKNOWLEDGEMENTS

We thank the Laria-Cimap (GANIL) and Mrs Guillamin for her contribution to ROS analysis at the SFR146 flow cytometry platform (University Caen Basse-Normandie). We acknowledge the contribution of the flow cytometry platform of the SFR BioSciences-Gerland-Lyon-Sud (UMS3444/US8) and of the CRCL. This work was supported by France Hadron (ANR-11-INBS-0007) and Labex Primes (ANR-11-LABX-0063).

CONFLICT OF INTEREST

The authors declare no conflict of interest.

REFERENCES

Antonovic L, Brahme A, Furusawa Y, Toma-Dasu I (2013) Radiobiological description of the LET dependence of the cell survival of oxic and anoxic cells irradiated by carbon ions. *J Radiat Res* **54**: 18–26.

Bertrand G, Maalouf M, Boivin A, Battiston-Montagne P, Beuve M, Levy A, Jalade P, Fournier C, Ardail D, Magné N, Alphonse G, Rodriguez-Lafrasse C (2014) Targeting head and neck cancer stem cells to overcome resistance to photon and carbon ion radiation. *Stem Cell Rev* **10**: 114–126.

Beuve M, Alphonse G, Maalouf M, Colliaux A, Battiston-Montagne P, Jalade P, Balanzat E, Demeyer A, Bajard M, Rodriguez-Lafrasse C (2008) Radiobiologic parameters and local effect model predictions for head-and-neck squamous cell carcinomas exposed to high linear energy transfer Ions. *Int J Radiat Oncol Biol*Phys* **71**: 635–642.

Boivin A, Hanot M, Malesys C, Maalouf M, Rousson R, Rodriguez-Lafrasse C, Ardail D (2011) Transient alteration of cellular redox buffering before irradiation triggers apoptosis in head and neck carcinoma stem and non-stem cells. *PLoS One* **6**: e14558.

Colliaux A, Gervais B, Rodriguez-Lafrasse C, Beuve M (2011) O 2 and glutathione effects on water radiolysis: a simulation study. *J Phys Conf Ser* **261**: 012007.

Das B, Tsuchida R, Malkin D, Koren G, Baruchel S, Yeger H (2008) Hypoxia enhances tumor stemness by increasing the invasive and tumorigenic side population fraction. *Stem Cells* **26**: 1818–1830.

Dettmering T, Zahnreich S, Colindres-Rojas M, Durante M, Taucher-Scholz G, Fournier C (2015) Increased effectiveness of carbon ions in the production of reactive oxygen species in normal human fibroblasts *J Radiat Res* **56**: 67–76.

Douki T, Ravanat J-L, Pouget J-P, Testard I, Cadet J (2006) Minor contribution of direct ionization to DNA base damage inducedby heavy ions. *Int J Radiat Biol* **82**: 119–127.

Durantel F, Balanzat E, Cassimi A, Chevalier F, Ngono-Ravache Y, Madi T, Poully J-C, Ramillon J-M, Rothard H, Ropars F, Schwob L, Testard I, Saintigny Y (2016) Dosimetry for radiobiology experiments at GANIL. *Nucl Instr Meth Phys Res* **816**: 70–77.

Fu Z, Chen D, Cheng H, Wang F (2015) Hypoxia-inducible factor-1α protects cervical carcinoma cells from apoptosis induced by radiation via modulation of vascular endothelial growth factor and p53 under hypoxia. *Med Sci Monit* **21**: 318–325.

Gilormini M, Wozny A-S, Battiston-Montagne P, Ardail D, Alphonse G, Rodriguez-Lafrasse C (2016) Isolation and characterization of a head and neck Squamous cell carcinoma subpopulation having stem cell characteristics. *J Vis Exp*; e-pub ahead of print 11 May 2016; doi:10.3791/53958.

Harada H, Itasaka S, Kizaka-Kondoh S, Shibuya K, Morinibu A, Shinomiya K, Hiraoka M (2009) The Akt/mTOR pathway assures the synthesis of HIF-1alpha protein in a glucose- and reoxygenation-dependent manner in irradiated tumors. *J Biol Chem* **284**: 5332–5342.

Jin Z, Aixi Y, Baiwen Q, Zonghuan L, Xiang H (2015) Inhibition of hypoxia-inducible factor-1 alpha radiosensitized MG-63 human osteosarcoma cells in vitro. *Tumori* **101**: 578–584.

Kamada T, Tsujii H, Blakely EA, Debus J, De Neve W, Durante M, Jäkel O, Mayer R, Orecchia R, Pötter R, Vatnitsky S, Chu WT (2015) Carbon ion

radiotherapy in Japan: an assessment of 20 years of clinical experience. *Lancet Oncol* **16**: e93–e100.
Ke Q, Costa M (2006) Hypoxia-inducible factor-1 (HIF-1). *Mol Pharmacol* **70**: 1469–1480.
Kim Y-H, Yoo K-C, Cui Y-H, Uddin N, Lim E-J, Kim M-J, Nam S-Y, Kim I-G, Suh Y, Lee S-J (2014) Radiation promotes malignant progression of glioma cells through HIF-1alpha stabilization. *Cancer Lett* **354**: 132–141.
Lapidot T, Sirard C, Vormoor J, Murdoch B, Hoang T, Caceres-Cortes J, Minden M, Paterson B, Caligiuri MA, Dick JE (1994) A cell initiating human acute myeloid leukaemia after transplantation into SCID mice. *Nature* **367**: 645–648.
Levin WP, Kooy H, Loeffler JS, DeLaney TF (2005) Proton beam therapy. *Br J Cancer* **93**: 849–854.
Li H, Wawrose JS, Gooding WE, Garraway LA, Lui VWY, Peyser ND, Grandis JR (2014) Genomic analysis of head and neck squamous cell carcinoma cell lines and human tumors: a rational approach to preclinical model selection. *Mol Cancer Res* **12**: 571–582.
Lu H, Samanta D, Xiang L, Zhang H, Hu H, Chen I, Bullen JW, Semenza GL (2015) Chemotherapy triggers HIF-1-dependent glutathione synthesis and copper chelation that induces the breast cancer stem cell phenotype. *Proc Natl Acad Sci USA* **112**: E4600–E4609.
Masoud GN, Li W (2015) HIF-1α pathway: role, regulation and intervention for cancer therapy. *Acta Pharm Sini B* **5**: 378–389.
Meesungnoen J, Jay-Gerin J-P (2009) High-LET ion radiolysis of water: oxygen production in tracks. *Radiat Res* **171**: 379–386.
Moncharmont C, Guy J-B, Wozny A-S, Gilormini M, Battiston-Montagne P, Ardail D, Beuve M, Alphonse G, Simoëns X, Rancoule C, Rodriguez-Lafrasse C, Magné N (2016) Carbon ion irradiation withstands cancer stem cells' migration/invasion process in Head and Neck Squamous Cell Carcinoma (HNSCC). *Oncotarget* **7**: 47738–47749.
Movafagh S, Crook S, Vo K (2015) Regulation of hypoxia-inducible factor-1a by reactive oxygen species: new developments in an old debate. *J Cell Biochem* **116**: 696–703.
Myszczyszyn A, Czarnecka AM, Matak D, Szymanski L, Lian F, Kornakiewicz A, Bartnik E, Kukwa W, Kieda C, Szczylik C (2015) The role of hypoxia and cancer stem cells in renal cell carcinoma pathogenesis. *Stem Cell Rev* **11**: 919–943.
Nordsmark M, Bentzen SM, Rudat V, Brizel D, Lartigau E, Stadler P, Becker A, Adam M, Molls M, Dunst J, Terris DJ, Overgaard J (2005) Prognostic value of tumor oxygenation in 397 head and neck tumors after primary radiation therapy. An international multi-center study. *Radiother Oncol* **77**: 18–24.
Ogata T, Teshima T, Inaoka M, Minami K, Tsuchiya T, Isono M, Furusawa Y, Matsuura N (2011) Carbon ion irradiation suppresses metastatic potential of human non-small cell lung cancer A549 cells through the phosphatidylinositol-3-kinase/Akt signaling pathway. *J Radiat Res* **52**: 374–379.
Peitzsch C, Perrin R, Hill RP, Dubrovska A, Kurth I (2014) Hypoxia as a biomarker for radioresistant cancer stem cells. *Int J Radiat Biol* **90**: 636–652.
Polyak K, Weinberg RA (2009) Transitions between epithelial and mesenchymal states: acquisition of malignant and stem cell traits. *Nat Rev Cancer* **9**: 265–273.
Prise KM, Folkard M, Newman HC, Michael BD (1994) Effect of radiation quality on lesion complexity in cellular DNA. *Int J Radiat Biol* **66**: 537–542.
Rankin EB, Giaccia AJ (2016) Hypoxic control of metastasis. *Science* **352**: 175–180.
Revel F, Gilbert T, Roche S, Drai J, Blond E, Ecochard R, Bonnefoy M (2015) Influence of oxidative stress biomarkers on cognitive decline. *J Alzheimers Dis* **45**: 553–560.
Rycaj K, Tang DG (2014) Cancer stem cells and radioresistance. *Int J Radiat Biol* **90**: 615–621.
Schlaff CD, Krauze A, Belard A, O'Connell JJ, Camphausen KA (2014) Bringing the heavy: carbon ion therapy in the radiobiological and clinical context. *Radiat Oncol* **9**: 88.
Semenza GL (2001) Hypoxia-inducible factor 1: oxygen homeostasis and disease pathophysiology. *Trends Mol Med* **7**: 345–350.
Seo EJ, Kim DK, Jang IH, Choi EJ, Shin SH, Lee SI, Kwon S-M, Kim K-H, Suh D-S, Kim JH (2016) Hypoxia-NOTCH1-SOX2 signaling is important for maintaining cancer stem cells in ovarian cancer. *Oncotarget* **7**: 55624–55638.
Shen C, Xiang M, Nie C, Hu H, Ma Y, Wu H (2013) CD44 as a molecular marker to screen cancer stem cells in hypopharyngeal cancer. *Acta Otolaryngol* **133**: 1219–1226.
Subtil FSB, Wilhelm J, Bill V, Westholt N, Rudolph S, Fischer J, Scheel S, Seay U, Fournier C, Taucher-Scholz G, Scholz M, Seeger W, Engenhart-Cabillic R, Rose F, Dahm-Daphi J, Hänze J (2014) Carbon ion radiotherapy of human lung cancer attenuates HIF-1 signaling and acts with considerably enhanced therapeutic efficiency. *FASEB J* **28**: 1412–1421.
Tinganelli W, Durante M, Hirayama R, Krämer M, Maier A, Kraft-Weyrather W, Furusawa Y, Friedrich T, Scifoni E (2015) Kill-painting of hypoxic tumours in charged particle therapy. *Sci Rep* **5**: 17016.
Tobias CA, Blakely EA, Alpen EL, Castro JR, Ainsworth EJ, Curtis SB, Ngo FQ, Rodriguez A, Roots RJ, Tenforde T, Yang TC (1982) Molecular and cellular radiobiology of heavy ions. *Int J Radiat Oncol Biol Phys* **8**: 2109–2120.
Tonissi F, Lattanzio L, Astesana V, Cavicchioli F, Ghiglia A, Monteverde M, Vivenza D, Gianello L, Russi E, Merlano M, Lo Nigro C (2016) Reoxygenation reverses hypoxia-related radioresistance in head and neck cancer cell lines. *Anticancer Res* **36**: 2211–2215.
Wang H, Zhang C, Xu L, Zang K, Ning Z, Jiang F, Chi H, Zhu X, Meng Z (2016) Bufalin suppresses hepatocellular carcinoma invasion and metastasis by targeting HIF-1α via the PI3K/AKT/mTOR pathway. *Oncotarget* **7**: 20193–20208.
Weijer R, Broekgaarden M, Krekorian M, Alles LK, van Wijk AC, Mackaaij C, Verheij J, van der Wal AC, van Gulik TM, Storm G, Heger M (2016) Inhibition of hypoxia inducible factor 1 and topoisomerase with acriflavine sensitizes perihilar cholangiocarcinomas to photodynamic therapy. *Oncotarget* **7**: 3341–3356.
Wenzl T, Wilkens JJ (2011) Modelling of the oxygen enhancement ratio for ion beam radiation therapy. *Phys Med Biol* **56**: 3251–3268.
Wulbrand C, Seidl C, Gaertner FC, Bruchertseifer F, Morgenstern A, Essler M, Senekowitsch-Schmidtke R (2013) Alpha-particle emitting 213Bi-anti-EGFR immunoconjugates eradicate tumor cells independent of oxygenation. *PLoS One* **8**: e64730.
Ye J, Wu D, Wu P, Chen Z, Huang J (2014) The cancer stem cell niche: cross talk between cancer stem cells and their microenvironment. *Tumour Biol* **35**: 3945–3951.

Supplementary Information accompanies this paper on British Journal of Cancer website (http://www.nature.com/bjc)